ADVANCED THERAPEUTICS
www.advtherap.com

Decellularized Extracellular Matrix Hydrogels as a Delivery Platform for MicroRNA and Extracellular Vesicle Therapeutics

*Melissa J. Hernandez, Roberto Gaetani, Vera M. Pieters, Nathan W. Ng, Audrey E. Chang, Taylor R. Martin, Eva van Ingen, Emma A. Mol, Monika Dzieciatkowska, Kirk C. Hansen, Joost P.G. Sluijter, and Karen L. Christman**

In the last decade, the use of microRNA (miRNA) and extracellular vesicle (EV) therapies has emerged as an alternative approach to mitigate the negative effects of several disease pathologies ranging from cancer to tissue and organ regeneration; however, delivery approaches toward target tissues have not been optimized. To alleviate these challenges, including rapid diffusion upon injection and susceptibility to degradation, porcine-derived decellularized extracellular matrix (ECM) hydrogels are examined as a potential delivery platform for miRNA and EV therapeutics. The incorporation of EVs and miRNA antagonists, including anti-miRs and antago-miRs, in ECM hydrogels results in a prolonged release as compared to the biologic agents alone. In addition, individual in vitro assessments confirm the bioactivity of the therapeutics upon release from the ECM hydrogels. This work demonstrates the feasibility of encapsulating miRNA and EV therapeutics in ECM hydrogels to enhance delivery and potentially efficacy in later in vivo applications.

1. Introduction

Therapeutics, particularly growth factor–based and cell-based, have been extensively investigated for many clinical applications including, but not limited to, cardiovascular disease,[1,2] cancer,[3,4] and autoimmune diseases.[5,6] With mechanisms regulating essential biological processes such as neovascularization, extracellular matrix remodeling, and inflammation, many growth factor–based and cell-based therapies have been pursued in clinical trials, but translation to the clinic has been largely unsuccessful.[7–9] Along with a lack of demonstrated efficacy in patients, manufacturing difficulties, like shortened shelf life and high production costs, hinder the feasibility of utilizing cell and growth factor–based approaches. Although engineered growth factors have recently been introduced to overcome many of these obstacles from growth factor therapeutics,[10,11] researchers have been exploring alternative biologics, including microRNAs (miRNAs) and extracellular vesicles (EVs).

MiRNAs, short 20–22 base pair oligonucleotides, have emerged as a promising therapeutic for many applications, including cardiovascular disease,[12] inflammatory disease,[13] metabolic disease,[14] and cancer.[15,16] These therapies harness the ability of miRNAs to regulate post-transcriptional gene expression, which occurs via complementary binding with a target messenger RNA. Chemical modifications have been implemented to produce miRNA mimics and inhibitors with increased stability and more favorable pharmacokinetics,[17,18] which have contributed to multiple miRNA therapeutics progressing to clinical trials.[19]

Another class of biologic products that is emerging as a potent cellular mediator in numerous physiological and pathological processes is EVs. EVs, cell-derived vesicles comprising

M. J. Hernandez, Dr. R. Gaetani, V. M. Pieters, N. W. Ng, A. E. Chang, T. R. Martin, E. van Ingen, Dr. K. L. Christman
Department of Bioengineering
Sanford Consortium for Regenerative Medicine
University of California, San Diego
La Jolla, CA, 92093, USA
E-mail: christman@eng.ucsd.edu
E. A. Mol
University Medical Center Utrecht
Experimental Cardiology Laboratory
University Utrecht
3584CX, Utrecht, The Netherlands
Dr. M. Dzieciatkowska, Dr. K. C. Hansen
Department of Biochemistry and Molecular Genetics
School of Medicine
University of Colorado
Aurora, CO, 80045, USA
Dr. J. P. G. Sluijter
University Medical Center Utrecht
Experimental Cardiology Laboratory
UMC Utrecht Regenerative Medicine Center
University Utrecht
3584CX, Utrecht, The Netherlands

DOI: 10.1002/adtp.201800032

exosomes and microvesicles, have been shown to play a major role in cell to cell communication, allowing cells to exchange proteins, lipids, and genetic materials, including mRNAs and noncoding RNAs such as miRNAs, thus making them effective regulators of tissue homeostasis and repair.[20,21] EVs have been shown to play a major role in many processes including cell signaling,[22,23] immunity,[5,24] cancer development and progression,[25,26] protein clearance,[27] and infection.[28,29] Due to their broad repertoire of bioactive molecules and biological functions,[21,30] EVs have been investigated in many therapeutic applications including organ regeneration,[30–32] cancer,[33,34] immune-based diseases,[35,36] and neurodegenerative diseases.[37]

Although miRNA and EV therapeutics have resulted in significant therapeutic outcomes in many preclinical studies,[19,38] these benefits are hindered by poor delivery strategies and rapid clearance soon after administration. Intravenous delivery is the main delivery route employed by these therapies, and direct injections have also been utilized; however, both of these approaches fail to capitalize on the full therapeutic potential of miRNAs and EVs. Current delivery methods, which often require large payloads, could yield undesired side effects from unspecific binding of miRNAs. In addition, degradation by endogenous nucleases and rapid diffusion represent significant obstacles.[12] Consequently, improved delivery strategies are greatly needed.

Several groups have begun exploring the use of hydrogels as a delivery platform for miRNA and EV therapies,[39,40] but natural materials alone (i.e., without the addition of chemical crosslinkers or modifications) have not been investigated. Unlike most synthetic materials, natural materials can better mimic the in vivo environment, but, in particular, decellularized extracellular matrix (ECM), one type of naturally derived biomaterial, successfully maintains biochemical cues of the native tissue microenvironment. Decellularized ECM has several beneficial properties, which include promoting cellular influx,[41] and its degradation products are angiogenic,[42] chemoattractant,[42,43] and promote cell migration and proliferation.[44] In addition, previous studies in a myocardial infarction model have confirmed the benefits of using cardiac-derived ECM hydrogels as a delivery platform for growth factors with increased arteriogenesis compared to growth factor alone and ECM hydrogel alone controls.[11,45] These ECM hydrogels have also been used for cell delivery in a hindlimb ischemia model of peripheral artery disease, which increased cell engraftment and survival, stimulated neovascularization and could also potentially be used for cell transplantation into the myocardium.[46,47] Along with the efficacy of these decellularized materials, the hydrogels can be delivered minimally invasively, as has been shown via catheter in the heart or a direct injection for the skeletal muscle.[46,48–50] With a complex mixture of proteins, we anticipated that an ample supply of binding sites would be present to facilitate the binding of nucleic acids and EVs. Additionally, ECM hydrogels could ensure localization of both miRNAs and EVs, and the nanoscale and microscale architecture of these hydrogels could promote a slow release of the payload.

Here we evaluated the use of porcine-derived decellularized ECM hydrogels as a platform for the delivery of model miRNAs and EVs (**Figure 1**). We performed assessments of our ECM hydrogels to provide a slow release profile and maintain bioactivity of miRNA and EV therapeutics, demonstrating that these biomaterials could be a potential delivery platform for such newer generation biologics.

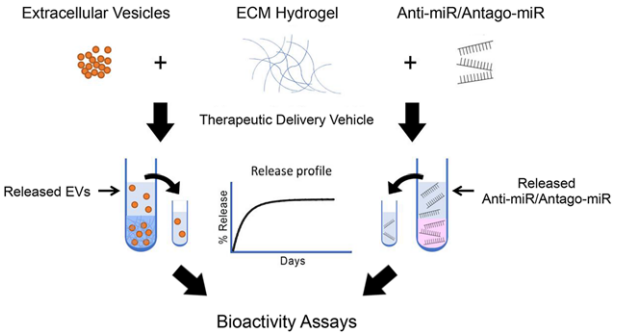

Figure 1. Schematic of the workflow for assessing decellularized ECM hydrogels as a delivery platform for miRNA and EV therapeutics. Anti-miRs, antago-miRs, and EVs were encapsulated in ECM hydrogels, and the release profiles were first generated. Antago-miR and EV release samples were then further analyzed to ensure the biologics remained bioactive.

2. Results and Discussion

Due to the earlier success with delivering growth factors and cells with tissue-derived hydrogels,[11,45–47] we hypothesized that the ECM hydrogels would also provide an enhanced delivery platform for model miRNAs and EVs. Specifically, we expected the ECM hydrogels would prolong the release of miRNAs and EVs but would not affect the bioactivity of either therapeutic. To first evaluate retention, model miRNAs and EVs were mixed with three different types of decellularized ECM hydrogels. Specifically, myocardial, skeletal muscle, and lung ECM hydrogels were used due to differences in the composition of ECM proteins[48,51] (Table S1, Supporting Information) and to demonstrate potential broad applications of this delivery platform. Although these hydrogels were derived from a xenogeneic tissue source, a very low amount of residual dsDNA was detected (Figure S1, Supporting Information), indicating adequate decellularization. Cardiac progenitor cell (CPC)-derived EVs[52] and miRNA antagonists for miR-214,[53] an anti-miR and antago-miR, were used as model therapeutics for these studies since they have been evaluated considerably and showed promising results in many therapeutic applications.[31,54,55]

2.1. MicroRNAs

For model miRNAs therapeutics, an anti-miR and antago-miR against miR-214 were used, which have been shown to recover neovascularization through the regulation of angiogenic factors.[53] Since decellularized ECM also has angiogenic properties,[42] this miRNA target was chosen since the combination of these therapies could potentially enhance neovascularization processes in later in vivo applications. The release profiles from the three ECM hydrogels were evaluated for the miRNA inhibitors up to 15 days (**Figure 2**). Comparing the anti-miR and antago-miR, the release profiles varied significantly, likely due to hydrophobic interactions caused by the presence of a

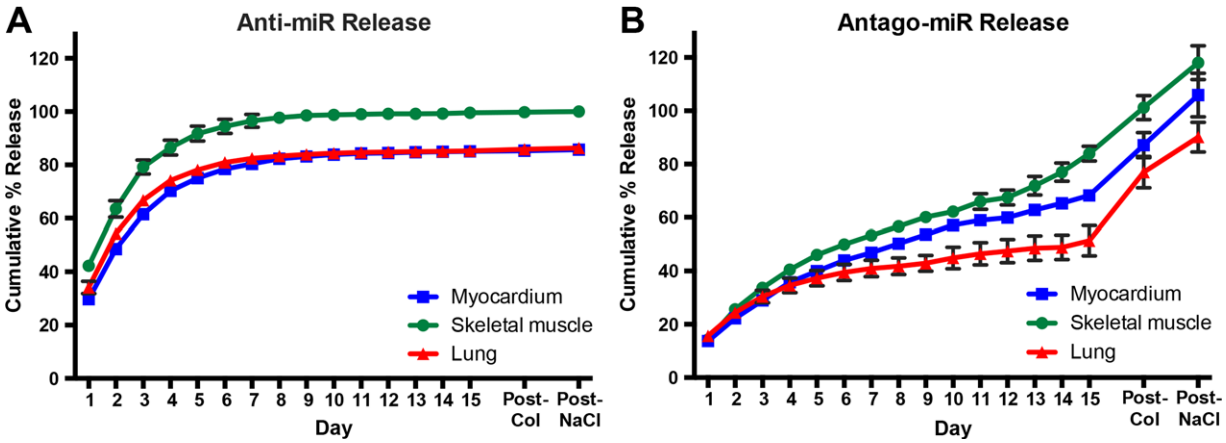

Figure 2. Release profiles for miRNA inhibitors of miR-214, an anti-miR and antago-miR. Values were obtained from fluorescence measurements using the Cy3 dye molecule conjugated to each miRNA. A) The anti-miR yielded a more rapid release rate, likely due to the absence of a cholesterol group, which is present on the antago-miR. B) The cholesterol group introduces hydrophobic interactions, which appear to affect the release rate. Some of the error bars are too small to be visualized at each time point. $n = 3$ per gel type. Data are mean ± SEM.

cholesterol group on the 3′ end of the antago-miR. In fact, over 50% of the anti-miR was released from the ECM hydrogels by day 2 (Figure 2A), but the antago-miR did not reach 50% until around day 10 (Figure 2B). Moreover, the anti-miR was virtually completely released by day 10, but the antago-miR was not fully released until the additions of first collagenase to degrade the collagen in the ECM hydrogels and then 1.5 M NaCl to dissociate residual antago-miRs. The rate of release was likely heavily facilitated by hydrophobic interactions, as indicated by the further release of antago-miR, but not anti-miR, following the addition of 1.5 M NaCl. The amount of amines present in the ECM hydrogels could also contribute to modulating the release profile, since there are some differences present amongst the tissue sources. Despite being very similar, the relative composition of the different ECM proteins differs among the different hydrogels (Table S1, Supporting Information). Specifically, the lung ECM hydrogel shows a broader composition of basement membrane proteins or different isoforms compared to the myocardial or skeletal muscle hydrogels, which in turn differ in the relative composition of the fibrillar collagen components. Moreover, the relative abundance of these ECM proteins, which was not investigated in the current study, could also play a fundamental role in regulating the release of the encapsulated therapeutic products.

Although some release profiles did not reach 100%, it is unlikely this was due to degradation since the chemical modifications made to the miRNA inhibitors provide added stability, and RNases-free solutions were used for all experiments. For those values above 100%, this was likely due to the gels slightly breaking down toward the end of the 15 days, particularly with the antago-miR, which may have resulted in samples containing larger amounts of the miRNA inhibitors. Unlabeled miRNA antagonists were also examined out to day 3 with the myocardial ECM hydrogel, which demonstrated that the Cy3 dye did not affect the release profiles (Figure S2, Supporting Information).

Since a prolonged release over a period of 1–2 weeks would likely be preferred, only the antago-miR was investigated for the in vitro studies. In addition, only the myocardial ECM hydrogel was studied further due to the relevance of this particular model miRNA inhibitor in applications of cardiovascular disease, like myocardial infarction. Although the incorporation of the antago-miR into the ECM hydrogels yielded prolonged release profiles, it was necessary to assess whether the ECM hydrogels interfered with the inherent bioactivity of the encapsulated antago-miR. To evaluate the bioactivity of the released antago-miRs, supernatant collected from myocardial ECM hydrogels at days 1 and 3 was tested in a Matrigel tube formation assay with human coronary artery endothelial cells (HCAECs), since miR-214 is known to affect angiogenic-related processes (**Figure 3**).[53] As a control, PBS supernatant obtained from hydrogels at day 15 was used since this likely contained the maximum amount of ECM soluble factors, which could also potentially have angiogenic effects. After incubating the cells with miRNA-conditioned media for 12 h, visual differences were observed in the degree of tube formation (Figure 3A). Compared to the PBS supernatant controls, released samples from days 1 and 3 yielded more organized tubes with significantly less cell clustering. When normalized to the PBS supernatant group, the total length increased to 1.53 ± 0.15 for day 1 and 1.42 ± 0.08 for day 3, and the number of junctions increased to 1.84 ± 0.12 and 1.71 ± 0.19 for days 1 and 3, respectively (Figure 3B). Although, the extent of tube formation did slightly decrease at day 3 relative to day 1, this was likely due to using a fixed amount of sample for each well, which contained less released antago-miR for day 3. These results demonstrated that the antago-miR largely maintained bioactivity following release from ECM hydrogels; however, it was not possible to determine what fraction of the antago-miRs remained bioactive. Further experiments would be necessary to investigate this.

Overall, the use of the ECM hydrogels prolonged the release of the miRNA inhibitors, particularly the antago-miR, without impairing the bioactivity. This slower release rate would likely be favored for many therapeutic applications, and antago-miRs have been engineered to enhance efficacy in vivo. Specifically, the conjugation of the cholesterol group is thought to increase cellular uptake and improve in vivo stability.[18,56] By combining this optimized biologic with a decellularized ECM hydrogel, the beneficial outcomes from these therapies could be further augmented.

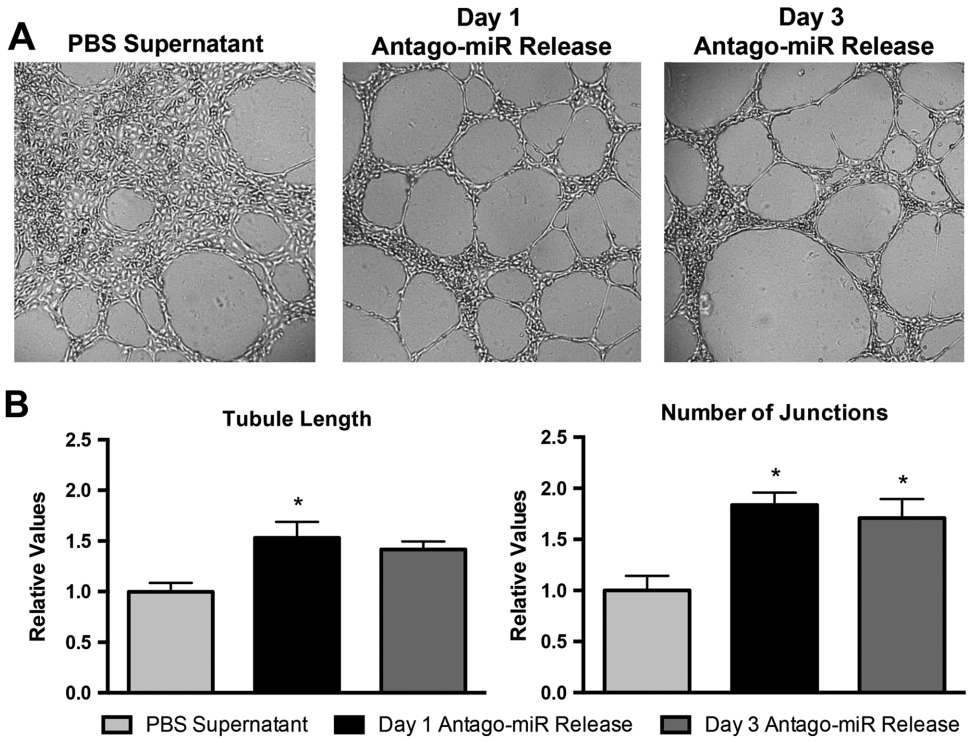

Figure 3. Bioactivity of released antago-miRs in a Matrigel tube formation assay. A) Representative images are shown for the tube formation of HCAECs on Matrigel. Since ECM soluble factors are present in the PBS supernatant group, some tube formation is seen but with a large degree of cell clustering. However, released samples from days 1 and 3 produce more organized tubes that yield relative increases in B) tubule length and the number of junctions over the PBS control ($n = 3$ per group). $^*p < 0.05$ compared to the PBS supernatant control using a one-way ANOVA with a Dunnett's post hoc test. Data are mean ± SEM.

2.2. Extracellular Vesicles

Similar to miRNAs, EVs have also been increasingly studied for many disease applications. In the present study, EVs derived from human cardiac progenitor cells (hCPCs)[52] were used for all experiments, as they have been shown to exert a protective effect on damaged myocardium by reducing cardiomyocyte apoptosis[55] and increasing cardiac function.[57] EVs were encapsulated into three different hydrogels and their release profile from the different scaffolds was evaluated at days 1, 3, and 7 (**Figure 4**). After 7 days, approximately 40%, 45%, and 25% of EVs were released from the myocardial, skeletal, and lung ECM hydrogels, respectively. Of the released EVs, the majority were detected 1 day after encapsulation, ranging from ≈30% in the myocardial and skeletal matrix hydrogels to ≈20% in the lung ECM hydrogels (Figure 4A). Most of the remaining EVs were released by day 3, and only a minimal increase was observed at day 7, indicating that a high amount of EVs were still retained in the gel. This was also indirectly confirmed by labeling the encapsulated EVs with PKH26 red fluorescent dye. A washing step after EV labeling and before EV encapsulation was also performed to remove excess dye, thus minimizing potential artifacts from free dye. The encapsulation of labeled EVs in the hydrogels conferred a pink coloration, which was still visible at the end of the release study, indicative of the presence of the encapsulated EVs (Figure 4B). We also quantified the remaining EVs by digesting the hydrogels with collagenase, confirming that indeed the majority of EVs were still encapsulated, with some differences among the different hydrogels. In particular, the cumulative study showed that after collagenase treatment, we were able to detect ≈80%, 70%, and 45% of the encapsulated EVs in the myocardial, skeletal, and lung ECM hydrogels, respectively. Since we were not able to detect all of the encapsulated EVs, we evaluated the effects of the collagenase treatment on EV detection shortly after encapsulation. EVs were encapsulated within the different hydrogels, and after hydrogel gelation, the gels were immediately treated with collagenase and compared with the same amount of nonencapsulated EVs. Our analysis showed that only ≈60% of the encapsulated EVs (58.75 ± 23.4%) were detected, indicating that the collagenase treatment negatively affected the EV detection, thus explaining the reason for not being able to recover all encapsulated EVs. However, we cannot exclude that some of the released EVs degraded due to experimental conditions, since it has been previously demonstrated that EVs are degraded when stored at 37 °C.[58] Moreover, since our detection method is based on CD63 expression on the EV membrane, it is possible that the expression of this receptor is influenced by our experimental conditions, thus affecting the total detection of the encapsulated EVs; however, this is unlikely. We also observed some degree of variability among different experiments when using the same tissue source. A possible reason could be due to slight differences in the ECM fibrous network between different experiments or potential differences in EV size between isolations, which could influence the kinetics of the EV release.

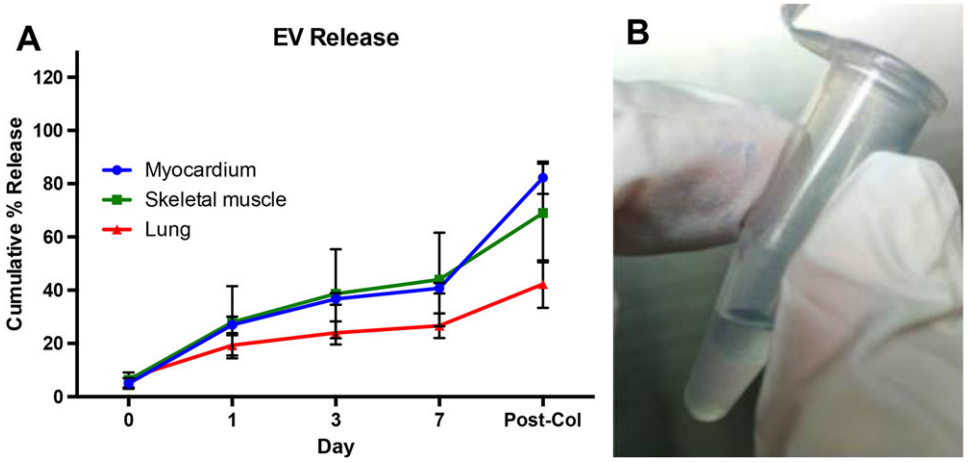

Figure 4. Cumulative release of hCPC-derived EVs from porcine ECM hydrogels. A) Conditioned PBS was collected at days 0, 1, 3, and 7, and the concentration of detected EVs is shown as a percentage of the mean fluorescent intensity of untreated EVs. Fluorescent intensities were determined with magnetic bead capture flow cytometry. Myocardial ECM hydrogels ($n = 4$), skeletal muscle ECM hydrogels ($n = 3$), and lung ECM hydrogels ($n = 3$) were examined. B) PKH26-labeled EVs confer a pink color to the gels, which is still visible after 7 days and indicates the presence of the encapsulated EVs. Data are mean ± SEM.

All ECM hydrogels provided a slow release of the encapsulated EV therapeutics; however, some differences were observed on the extent of the EV release between the different tissue sources. The level of released EVs detected in the EV-conditioned media from the lung ECM hydrogels was considerably lower than the values of the myocardial ECM and the skeletal muscle ECM hydrogels. A possible explanation could be that the composition of the lung ECM hydrogels allowed for a more sustained encapsulation of the EVs compared to the muscle tissue–derived ECM hydrogels. It is possible that a combination of physical entrapment, non-covalent interactions, or specific binding domains all contributed to the release profile of the encapsulated EVs. The combination of tissue-specific ECM molecules (Table S1, Supporting Information), which can affect the mechanical properties, pore size, and electrostatic properties of the hydrogel, could explain the differences observed among the different tissue sources.[59] Another possible mechanism behind the rate of EV release from the ECM hydrogels is the presence of matrix metalloproteinases (MMPs) in cardiac progenitor cell-derived extracellular vesicles.[60] These enzymes are generally known to induce ECM remodeling by degrading certain ECM molecules, which could modulate the degradation rate of ECM hydrogels in vivo.

We next evaluated if encapsulation could negatively impact the bioactivity of the released EVs and if the released EVs would still assert their beneficial effects once released from the hydrogels. Conditioned media from EVs encapsulated in hydrogels was used to stimulate the phosphorylation of the ERK 1/2 pathway in target HCAECs and compared to the PBS supernatant collected from empty hydrogels. Western blot analysis showed that the EVs released 1 and 3 days after encapsulation significantly increased the phosphorylation of the ERK 1/2 proteins when compared to the PBS supernatant controls (1.33 ± 0.07 and 1.42 ± 0.09 fold increase, respectively), and a trend was seen when the EV-conditioned media collected 7 days after encapsulation was used (1.43 ± 0.11 fold increase, $p = 0.058$; **Figure 5**). The reduced bioactivity of the released EVs 1 week after encapsulation could likely be due to the lower amount of EVs released after the first days. However, the minimal observed release or reduced bioactivity of the EV-conditioned media released at day 7 could also partly be due to EV degradation in the experimental conditions, as mentioned earlier.

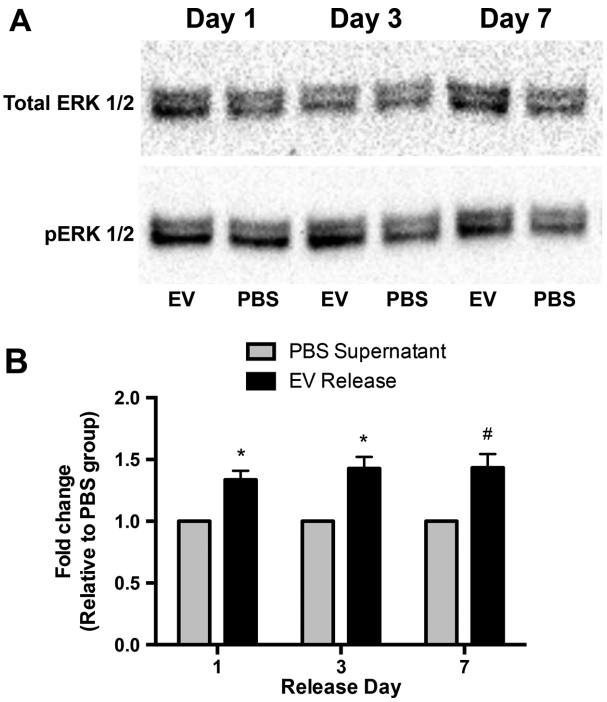

Figure 5. The effect of CPC-derived EVs released from myocardial ECM hydrogels on pERK 1/2 levels in HCAECs. Cells were incubated with conditioned PBS collected at days 1 ($n = 3$ per group), 3 ($n = 3$ per group), and 7 ($n = 3$ per group). The expression of pERK 1/2 was determined with A) western blot analysis and B) normalized to total ERK content and relative to conditioned PBS from empty ECM hydrogels. $*p < 0.05$ and $\#p = 0.059$ compared to PBS supernatant using an unpaired Student's *t*-test. Data are mean ± SEM.

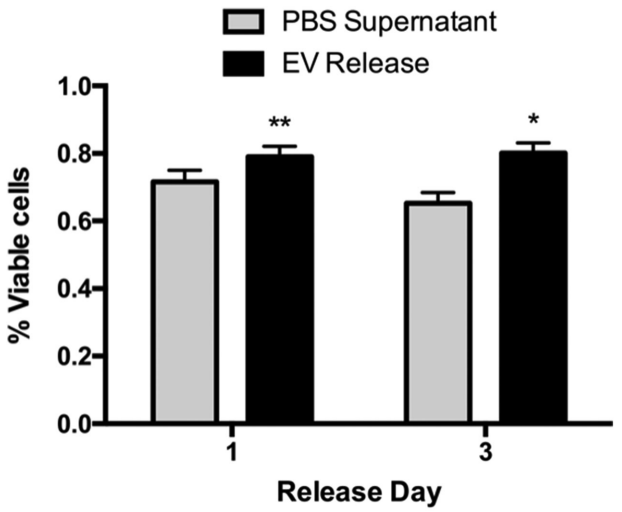

Figure 6. The protective effect of CPC-derived EVs released from myocardial ECM hydrogels on H_2O_2-induced apoptosis of hCPCs. Cells were incubated with conditioned PBS, collected at days 1 ($n = 6$ per group) and 3 ($n = 7$ per group) in combination with 25 μM H_2O_2. The survival rate was determined with an alamarBlue cell viability assay and normalized to alamarBlue baseline values. $*p < 0.05$ and $**p < 0.01$ compared to PBS supernatant using an unpaired Student's *t*-test. Data are mean ± SEM.

Since the EVs' therapeutic efficacy is in part mediated by exerting antiapoptotic effects on the targeted cells,[61] we then investigated whether released EVs were also able to preserve cell survival in the presence of reactive oxygen species. Based on the pERK activation data, we only evaluated EVs released 1 and 3 days after encapsulation. A significant increase in cell survival was observed with both EV-conditioned medias when compared to the PBS supernatants (EVs: 79.07 ± 3.03% at day 1 and 80.08 ± 3.06% at day 3; PBS: 71.64 ± 3.40% at day 1 and 65.26 ± 3.22% at day 3; **Figure 6**). The modest increase in cell survival observed using EVs released after 1 day could be explained by the protective effects also exerted by the hydrogel alone, as has been previously shown both in vitro[47] and in vivo[62]. It is possible that small ECM molecules that do not form the fibrous network of the hydrogel were released soon after PBS incubation, thus mitigating the pro-survival effects observed using EVs released 1 day after encapsulation.

3. Conclusion and Outlook

The discovery of miRNAs and EVs as potent mediators of cellular function and tissue homeostasis has led many researchers to investigate their potential use for a wide variety of disease pathways. However, similar to cells, growth factors, or small molecules, their delivery is hampered by rapid clearance soon after administration, therefore potentially limiting their therapeutic effects. The use of decellularized ECM hydrogels has been proposed as an alternative approach to modulate the release rate of model miRNA and EV therapeutics. Our data collectively indicated that these hydrogels successfully retained the encapsulated biologics over a prolonged period of time with some differences between the therapeutics or hydrogel tissue source. Samples collected for the release profiles were also further investigated with bioactivity assays, and both the antago-miR and EVs remained bioactive after being released from the ECM hydrogels. This study demonstrates that decellularized ECM hydrogels may represent a platform for slow delivery of miRNAs and EVs due to their ability to induce a pro-regenerative response in the damaged tissue, the possibility of utilizing minimally invasive catheter delivery, and an established path to clinical translation. Since the myocardial ECM hydrogel has already been injected via catheter in the hearts of myocardial infarction patients in a Phase I trial (clinicaltrials.gov identifier NCT02305602), and several other xenogeneic ECM products have been safely used in patients,[63,64] this suggests the clinical applicability of using injectable ECM hydrogels to deliver miRNAs and EVs in a wide array of disease applications.

4. Experimental Section

Extracellular Matrix Preparation: Porcine-derived extracellular matrix (ECM) was prepared as previously described.[51,65] Briefly, tissue from Yorkshire farm pigs was chopped into small cubes (2–5 mm) and decellularized with detergent for 3–5 days. Myocardial ECM, skeletal muscle ECM, and lung ECM was derived from porcine left ventricular myocardium, psoas muscle, and lung, respectively. For both the myocardial and skeletal muscle ECM hydrogels, decellularization was accomplished using 1% sodium dodecyl sulfate, while lung ECM hydrogels were decellularized with 0.1% sodium dodecyl sulfate. Skeletal muscle ECM hydrogels also required an additional isopropyl alcohol step to remove remaining lipids. Following decellularization, the tissue was then lyophilized and milled into a fine powder for long-term storage. Prior to use, the milled powder was partially digested with pepsin (Sigma-Aldrich) at a concentration of 10 mg ECM per 1 mL pepsin solution (1 mg pepsin per 1 mL 0.1 M HCl) for at least 48 h and then neutralized to physiological pH and salt conditions. Finally, the concentration of the ECM hydrogel was adjusted to 6 mg mL^{-1} with 1× phosphate buffered saline (PBS) and then lyophilized once again for storage at −80 °C.

Cell Culture: All cell lines were preserved in a humidified incubator at 37 °C, 5% CO_2 and atmospheric O_2. Human cardiac progenitor cells (hCPCs)[60] and human coronary artery endothelial cells (HCAECs) were used between passages 17–23 and 7–14, respectively. hCPCs were cultured as previously described.[66] Briefly, cells were cultured in 0.1% porcine gelatin (Sigma-Aldrich) coated flasks in growth media consisting of 10% fetal bovine serum (Thermo Fisher Scientific), 22% EBM2 (Lonza) complemented with EGM2 single quotes (Lonza) in Medium 199 (Corning), 1× nonessential amino acids (Lonza), and 1× penicillin-streptomycin (Life Technologies). HCAECs were grown in MesoEndo cell growth media (Cell Applications).

MiRNA Preparation: Anti-miR and antago-miR oligonucleotides were synthesized with the following sequence: 5′ – ACU GCC UGU CUG UGC CUG CUG T – 3′ (Eurofins Genomics). Both oligonucleotides were designed with 2′ O-methylation, 4 PTO-linkages on the 3′ end, and 2 PTO-linkages on the 5′ end. The antago-miR was further modified with a 3′ cholesterol group. For release experiments requiring miRNA detection via fluorescence measurements, a Cy3 dye molecule was conjugated to the 5′ end. All lyophilized anti-miR or antago-miR aliquots were resuspended with RNase-free water (Life Technologies) to a final concentration of 100 μM.

Anti-miR and Antago-miR Release: Decellularized ECM hydrogels were prepared by resuspending lyophilized aliquots to a final concentration of 6 mg mL^{-1} with RNase-free water or a mixture of RNase-free water and miRNA inhibitors. Cy3-labeled anti-miR (4 μg, $n = 3$ per ECM type) or antago-miR (4 μg, $n = 3$ per ECM type) was mixed into the ECM hydrogels.[53] Hydrogels (200 μL total) were formed in microcentrifuge tubes by incubating at 37 °C overnight. Larger volume gels were used for

the anti-miR and antago-miR release compared to the EVs release, since concentrated amounts of the antago-miR did affect gelation in vitro. All ECM hydrogels were initially rinsed with RNase-free 1× PBS (250 μL, Alfa Aesar) to remove any unincorporated anti-miR or antago-miR. After RNase-free 1× PBS (250 μL) was added to each gel, all gels were incubated at 37 °C on a shaker plate. Every 24 ± 2 h for 15 days, the PBS supernatant (200 μL) was collected for quantification of miRNA release. On day 15 following collection of the PBS supernatant, bacterial collagenase (200 μL, Worthington Biomedical Corporation) at 100 U mL^{-1} in a 0.1 M Tris-base, 0.25 M $CaCl_2$ solution, pH 7.4 was added to degrade the hydrogels. For complete degradation, gels were incubated at 37 °C for 4 h. Then, collagenase samples (200 μL) were collected, and 1.5 M NaCl solution (200 μL) was added to dissociate residual electrostatic interactions between the miRNAs and ECM hydrogels. Gels were allowed to incubate at 37 °C for 1 h prior to sample collection. The miRNA content in each of the release samples was quantified using a BioTek Synergy 4 Multi-Mode Microplate Reader. The Cy3 dye molecules were detected using an emission spectrum with a constant excitation at 547 nm and an emission ranging from 577 to 597 nm. Known amounts of the Cy3-labeled anti-miR or antago-miR were mixed with supernatant from empty ECM hydrogels to construct individual standard curves. These standard curves were then used to determine the amount of released miRNAs. Release samples were stored at −80 °C for later analysis.

Antago-miR Bioactivity—Tube Formation Assay: Growth factor reduced Matrigel (10 μL, Corning) was carefully pipetted into individual wells in a μ-slide angiogenesis (Ibidi) and allowed to gel at 37 °C for approximately 45 min. In the meantime, HCAECs were collected, and the mixture was then concentrated to 400 000 cells per mL in MesoEndo growth media for a total amount of 10 000 cells per well. In separate microcentrifuge tubes, samples were prepared to yield 50 μL total per well. Each sample tube contained sample (25 μL) and cells in media (25 μL). The sample volume was taken directly from tubes containing the collected release from days 1 and 3 and the PBS supernatant at day 15 prior to collagenase and 1.5 M NaCl treatments. The experiment was done in triplicate, and data was analyzed using the MATLAB AngioQuant toolbox.

EV Isolation: hCPCs from three different donors were used for EV isolation. CPCs were cultured in EV-free growth media until 80% confluency was reached, and the media was collected for EV isolation. To prepare EV-free growth media, 33% FBS in Medium 199 was centrifuged at 100 000 × *g* for 16 h at 4 °C (Optima L-80 XP Ultracentrifuge) and sterile filtered. The supernatant was used to prepare growth media as described earlier. hCPC-conditioned media was collected and centrifuged at 2000 × *g* for 15 min at 4 °C (Eppendorf Centrifuge 5810R) to pellet dead cells and debris. The supernatant was then centrifuged at 10 000 × *g* for 30 min at 4 °C to pellet larger vesicles. The EV pellet was obtained in the last centrifuge step at 100 000 × *g* at 4 °C for 60 min, sterile filtered, resuspended in PBS, and stored at 4 °C when used the next day or at −80 °C for long-term storage. EV concentration was measured using the Micro BCA Protein Assay Kit (Thermo Scientific). Bovine serum albumin (BSA) standards were prepared within the range of 0.5 μg mL^{-1} to 200 μg mL^{-1}. Both standards and EV samples were incubated with Micro BCA Working Reagent at 37 °C for 2 h and analyzed with a BioTek Synergy 4 Multi-Mode Microplate Reader at 562 nm. EV concentration was determined by comparing the values of the EV samples with the known concentrations of the standards.

EV Labeling: EVs were fluorescently labeled with 2 × 10^{-6} M PKH26 red fluorescent dye (Sigma; PKH26 Red Fluorescent cell linker mini-kit for general cell membrane labeling, MINI26-1KT) according to the manufacturer's protocol. The labeling reaction was stopped by adding 33% EV-free FBS in M199 (3 mL) and ultracentrifuged as described earlier. After centrifugation, the pellet was resuspended in PBS at a concentration of 0.5 μg μL^{-1} and used for encapsulation experiments.

EV Detection: EV release from decellularized myocardial ($n = 4$), skeletal muscle ($n = 3$), and lung ($n = 3$) ECM hydrogels was measured using an EV capture method with antibody-coated magnetic beads. Samples were incubated with anti-CD63-coated magnetic beads (ExoCap, JSR Life Sciences) overnight and washed by aspiration on the magnet and adding 2% BSA in PBS (washing buffer). Secondary CD63-Alexa647 antibody in PBS (BD Biosciences) was added and incubated for 2 h at room temperature while shaking. Beads were washed with washing buffer and resuspended in 0.25% BSA in PBS. Mean fluorescent intensity of the samples was measured by FACS (Canto).

EV Bioactivity—Stimulation of pERK Expression: In a flat bottom 24 well plate, 100 000 HCAECs were plated in MesoEndo cell growth media. After 24 h, the cells were starved by replacing media with Medium 199 for 3 h. Following starvation, HCAECs were incubated with myocardial ECM hydrogel-conditioned PBS (200 μL) from gels with or without encapsulated EVs. Samples from days 1 ($n = 4$ per group), 3 ($n = 3$ per group), and 7 ($n = 4$ per group) were examined. Cells were lysed with cOmplete Lysis-M buffer (Roche) on ice for 5 min. Lysate was centrifuged at 14 000 × *g* for 10 min at 4 °C, and the supernatant was stored at −80 °C. To prepare the samples for gel electrophoresis, HCAEC lysate (24 μL) was combined with 4× NuPAGE LDS Sample Buffer (10 μL, Thermo Fisher Scientific) and 10× NuPAGE Sample Reducing Agent (4 μL, Thermo Fisher Scientific). The samples were then heated for 10 min at 70 °C. A NuPAGE 4–12% Bis-Tris Protein Gel (Thermo Fisher Scientific) was loaded with sample (40 μL) and PageRuler Prestained Protein Ladder (15 μL, Thermo Fisher Scientific). The gel was placed in the XCell SureLock Mini-Cell Electrophoresis System (Thermo Fisher Scientific), and the chambers were filled with 1× NuPAGE MOPS SDS Running Buffer (Thermo Fisher Scientific). In addition, NuPAGE Antioxidant (500 μL, Thermo Fisher Scientific) was added to the inner chamber. Electrophoresis was performed at 200 volts for 50 min. Western blot was performed using the XCell SureLock Mini-Cell Electrophoresis System filled with 1× NuPAGE Transfer Buffer (Thermo Fisher Scientific) in 10% methanol in deionized water. Proteins were transferred from the gel onto a 0.45 μm nitrocellulose membrane (Bio-Rad Laboratories) at 35 volts for 1 h on ice. The membrane was blocked in 5% BSA (Gemini Bio) in TBS for 1 h at room temperature, followed by incubation with primary antibodies 1:500 phospho-p44/42 MAPK (Thr202/Tyr204; Cell Signal) or 1:750 p42/44 MAPK (ERK1/2; Cell Signaling Technology) in 0.5% BSA in TBS for 1 h at room temperature. The membrane was then incubated with secondary antibody 1:1000 goat anti-rabbit IgG HRP (Abcam) in 5% milk 0.1% Tween in TBS for 1 h at room temperature. Prior to imaging, the membrane was incubated with Pierce ECL Western Blotting Substrate (Thermo Fisher Scientific) for 1 min and imaged with a Bio-Rad ChemiDoc MP System using Image Lab 3.0 software. Total ERK was evaluated on the same membrane used for phospho-p44/42 MAPK. To remove primary and secondary pERK antibodies, the membrane was incubated in stripping buffer (1.5% glycine, 0.1% SDS, 1% Tween 20 in H_2O at pH 2.2; 2 × 7.5 min) followed by washing in PBS (2 × 10 min) and TBS (2 × 10 min) and stained as described earlier.

EV Bioactivity—Antiapoptotic Effect: A 96-well plate was coated with 0.1% porcine gelatin, and 7500 hCPCs per well were seeded and incubated in growth media overnight. After 24 h, the media was replaced by 10% alamarBlue Cell Viability Reagent (Invitrogen) in growth media and incubated for 4 h at 37 °C. AlamarBlue was transferred to a flat bottom 96-well plate (100 μL per well), and baseline values were measured in a BioTek Synergy 4 Multi-Mode Microplate Reader at 550 nm excitation and 585 nm emission. After baseline measurements, cells were incubated with 25 μM H_2O_2 in myocardial ECM hydrogel-conditioned PBS from gels with or without encapsulated EVs for 16 h at 37 °C followed by incubation with 10% alamarBlue in growth media for 4 h at 37 °C. AlamarBlue was again transferred to a flat bottom 96-well plate (100 μL per well), and the final values were measured with the microplate reader.

Statistical Analysis: Results are displayed as mean ± standard error of the mean (SEM). GraphPad Prism 6 was used for statistical analyses with significance accepted at $p < 0.05$ for all experiments. For the miRNA release experiments, individual standard curves were generated each day for the anti-miR and antago-miR using PBS supernatant collected from empty ECM hydrogels. The amount of miRNA rinsed away on day 0 was subtracted from the original 4 μg and used as the total amount for calculating the cumulative percent released. Some of the error bars are too small to be seen on the miRNA release study graphs. A sample size of three gels was used for both miRNA antagonists and each ECM type (18 gels total). Images taken for assessing the bioactivity of the released antagomiRs were analyzed with the MATLAB AngioQuant toolbox. Each experimental group was done in triplicate, and values for the tubule length and

number of junctions were normalized to the PBS supernatant group. For comparisons between the antago-miR release samples and PBS supernatant control, a one-way ANOVA with a Dunnett's post hoc test was used. For the EV release study, standard curves were generated using known amounts of EVs, and EV detection was done as described previously. A total of four hydrogels were evaluated for the myocardial ECM, and three hydrogels were tested for the skeletal muscle and lung ECM. To analyze the results from the pERK expression studies, ImageJ software was utilized to quantify the intensity of the bands ($n = 3$ per group for day 3, $n = 4$ per group for days 1 and 7) with respect to total ERK. Values were normalized to the PBS supernatant group for each time point and then compared with an unpaired Student's *t*-test. Cell survival for the apoptosis experiment was measured as percentage of viable cells compared to baseline measurements. Six and seven replicates were performed for day 1 and day 3 samples, respectively. An unpaired Student's *t*-test was used to determine statistical significance.

Supporting Information

Supporting Information is available from the Wiley Online Library or from the author.

Acknowledgements

M.J.H. and R.G. contributed equally to this work. This work was supported by the NIH NHLBI (R01HL113468). M.J.H. was supported by the NHLBI (F31HL132584, T32HL105373). J.P.G.S. and E.M. are supported by Horizon2020 ERC-2016-COG EVICARE (725229), the Project SMARTCARE-II of the BioMedicalMaterials Institute, co-funded by the ZonMw-TAS program (#116002016), the Dutch Ministry of Economic Affairs, Agriculture and Innovation and the Netherlands CardioVascular Research Initiative (CVON): the Dutch Heart Foundation, Dutch Federations of University Medical Centers, the Netherlands Organization for Health Research and Development, and the Royal Netherlands Academy of Sciences.

Conflict of Interest

K.L.C. is co-founder, consultant, board member, and holds equity interest in Ventrix, Inc.

Keywords

extracellular matrix, extracellular vesicles, hydrogels, microRNAs

Received: March 7, 2018
Revised: April 9, 2018
Published online: May 28, 2018

[1] V. F. Segers, R. T. Lee, *Nature* **2008**, *451*, 937.
[2] C. L. Hastings, E. T. Roche, E. Ruiz-Hernandez, K. Schenke-Layland, C. J. Walsh, G. P. Duffy, *Adv. Drug. Deliv. Rev.* **2015**, *84*, 85.
[3] J. R. Woodburn, *Pharmacol. Ther.* **1999**, *82*, 241.
[4] S. Tugues, S. Koch, L. Gualandi, X. Li, L. Claesson-Welsh, *Mol. Aspects Med.* **2011**, *32*, 88.
[5] P. D. Robbins, A. E. Morelli, *Nat. Rev. Immunol.* **2014**, *14*, 195.
[6] H. Munir, H. M. McGettrick, *Stem. Cells Dev.* **2015**, *24*, 2091.
[7] A. Trounson, C. McDonald, *Cell Stem Cell* **2015**, *17*, 11.
[8] D. A. M. Feyen, R. Gaetani, P. A. Doevendans, J. P. G. Sluijter, *Adv. Drug. Deliv. Rev.* **2016**, *106*, 104.
[9] J. P. G. Sluijter, S. M. Davidson, C. M. Boulanger, E. I. Buzas, D. P. V. de Kleijn, F. B. Engel, Z. Giricz, D. J. Hausenloy, R. Kishore, S. Lecour, J. Leor, R. Madonna, C. Perrino, F. Prunier, S. Sahoo, R. M. Schiffelers, R. Schulz, L. W. Van Laake, K. Ytrehus, P. Ferdinandy, *Cardiovasc. Res.* **2018**, *114*, 19.
[10] C. J. Liu, D. S. Jones, 2nd, P. C. Tsai, A. Venkataramana, J. R. Cochran, *FEBS Lett.* **2014**, *588*, 4831.
[11] S. B. Sonnenberg, A. A. Rane, C. J. Liu, N. Rao, G. Agmon, S. Suarez, R. Wang, A. Munoz, V. Bajaj, S. Zhang, R. Braden, P. J. Schup-Magoffin, O. L. Kwan, A. N. DeMaria, J. R. Cochran, K. L. Christman, *Biomaterials* **2015**, *45*, 56.
[12] E. van Rooij, E. N. Olson, *Nat. Rev. Drug Discov.* **2012**, *11*, 860.
[13] R. Dai, S. A. Ahmed, *Transl. Res.* **2011**, *157*, 163.
[14] V. Rottiers, A. M. Naar, *Nat. Rev. Mol. Cell Biol.* **2012**, *13*, 239.
[15] Y. Chen, D. Y. Gao, L. Huang, *Adv. Drug. Deliv. Rev.* **2015**, *81*, 128.
[16] A. L. Kasinski, F. J. Slack, *Nat. Rev. Cancer* **2011**, *11*, 849.
[17] K. A. Lennox, M. A. Behlke, *Gene Ther.* **2011**, *18*, 1111.
[18] J. Krutzfeldt, N. Rajewsky, R. Braich, K. G. Rajeev, T. Tuschl, M. Manoharan, M. Stoffel, *Nature* **2005**, *438*, 685.
[19] E. van Rooij, A. L. Purcell, A. A. Levin, *Circ. Res.* **2012**, *110*, 496.
[20] J. M. Pitt, G. Kroemer, L. Zitvogel, *J. Clin. Invest.* **2016**, *126*, 1139.
[21] G. van Niel, G. D'Angelo, G. Raposo, *Nat. Rev. Mol. Cell Biol.* **2018**, *19*, 213.
[22] H. Valadi, K. Ekstrom, A. Bossios, M. Sjostrand, J. J. Lee, J. O. Lotvall, *Nat. Cell Biol.* **2007**, *9*, 654.
[23] C. Cossetti, N. Iraci, T. R. Mercer, T. Leonardi, E. Alpi, D. Drago, C. Alfaro-Cervello, H. K. Saini, M. P. Davis, J. Schaeffer, B. Vega, M. Stefanini, C. Zhao, W. Muller, J. M. Garcia-Verdugo, S. Mathivanan, A. Bachi, A. J. Enright, J. S. Mattick, S. Pluchino, *Mol. Cell* **2014**, *56*, 193.
[24] P. D. Robbins, A. Dorronsoro, C. N. Booker, *J. Clin. Invest.* **2016**, *126*, 1173.
[25] N. Kosaka, Y. Yoshioka, Y. Fujita, T. Ochiya, *J. Clin. Invest.* **2016**, *126*, 1163.
[26] Y. Naito, Y. Yoshioka, Y. Yamamoto, T. Ochiya, *Cell. Mol. Life Sci.* **2017**, *74*, 697.
[27] K. Yuyama, H. Sun, S. Mitsutake, Y. Igarashi, *J. Biol. Chem.* **2012**, *287*, 10977.
[28] T. N. Bukong, F. Momen-Heravi, K. Kodys, S. Bala, G. Szabo, *PLoS Pathog.* **2014**, *10*, e1004424.
[29] R. D. Wiley, S. Gummuluru, *Proc. Natl. Acad. Sci. U.S.A.* **2006**, *103*, 738.
[30] S. E. L. Andaloussi, I. Mager, X. O. Breakefield, M. J. Wood, *Nat. Rev. Drug Discov.* **2013**, *12*, 347.
[31] E. A. Mol, M. J. Goumans, J. P. G. Sluijter, *Adv. Exp. Med. Biol.* **2017**, *998*, 207.
[32] H. Jing, X. He, J. Zheng, *Transl. Res.* **2018**. https://doi.org/10.1016/j.trsl.2018.01.005
[33] J. A. Tickner, A. J. Urquhart, S. A. Stephenson, D. J. Richard, K. J. O'Byrne, *Front Oncol.* **2014**, *4*, 127.
[34] P. Vader, X. O. Breakefield, M. J. Wood, *Trends Mol. Med.* **2014**, *20*, 385.
[35] V. Borger, M. Bremer, R. Ferrer-Tur, L. Gockeln, O. Stambouli, A. Becic, B. Giebel, *Int. J. Mol. Sci.* **2017**, *18*.
[36] L. Tan, H. Wu, Y. Liu, M. Zhao, D. Li, Q. Lu, *Autoimmunity* **2016**, *49*, 357.
[37] C. Quek, A. F. Hill, *Biochem. Biophys. Res. Commun.* **2017**, *483*, 1178.
[38] C. Akyurekli, Y. Le, R. B. Richardson, D. Fergusson, J. Tay, D. S. Allan, *Stem Cell Rev.* **2015**, *11*, 150.
[39] M. J. Hernandez, K. L. Christman, *JACC Basic Transl. Sci.* **2017**, *2*, 212.
[40] C. M. Curtin, I. M. Castano, F. J. O'Brien, *Adv. Healthc. Mater.* **2018**, *7*.
[41] E. Rieder, A. Nigisch, B. Dekan, M. T. Kasimir, F. Muhlbacher, E. Wolner, P. Simon, G. Weigel, *Biomaterials* **2006**, *27*, 5634.
[42] F. Li, W. Li, S. Johnson, D. Ingram, M. Yoder, S. Badylak, *Endothelium* **2004**, *11*, 199.
[43] A. J. Beattie, T. W. Gilbert, J. P. Guyot, A. J. Yates, S. F. Badylak, *Tissue Eng. Part A* **2009**, *15*, 1119.

[44] J. E. Reing, L. Zhang, J. Myers-Irvin, K. E. Cordero, D. O. Freytes, E. Heber-Katz, K. Bedelbaeva, D. McIntosh, A. Dewilde, S. J. Braunhut, S. F. Badylak, *Tissue Eng. Part A* **2009**, *15*, 605.
[45] S. B. Seif-Naraghi, D. Horn, P. J. Schup-Magoffin, K. L. Christman, *Acta Biomater.* **2012**, *8*, 3695.
[46] N. Rao, G. Agmon, M. T. Tierney, J. L. Ungerleider, R. L. Braden, A. Sacco, K. L. Christman, *ACS Nano.* **2017**, *11*, 3851.
[47] R. Gaetani, C. Yin, N. Srikumar, R. Braden, P. A. Doevendans, J. P. Sluijter, K. L. Christman, *Cell Transplant.* **2016**, *25*, 1653.
[48] J. L. Ungerleider, T. D. Johnson, M. J. Hernandez, D. I. Elhag, R. L. Braden, M. Dzieciatkowska, K. G. Osborn, K. C. Hansen, E. Mahmud, K. L. Christman, *JACC Basic Trans. Sci.* **2016**, *1*, 32.
[49] J. M. Singelyn, P. Sundaramurthy, T. D. Johnson, P. J. Schup-Magoffin, D. P. Hu, D. M. Faulk, J. Wang, K. M. Mayle, K. Bartels, M. Salvatore, A. M. Kinsey, A. N. Demaria, N. Dib, K. L. Christman, *J. Am. Coll. Cardiol.* **2012**, *59*, 751.
[50] S. B. Seif-Naraghi, J. M. Singelyn, M. A. Salvatore, K. G. Osborn, J. J. Wang, U. Sampat, O. L. Kwan, G. M. Strachan, J. Wong, P. J. Schup-Magoffin, R. L. Braden, K. Bartels, J. A. DeQuach, M. Preul, A. M. Kinsey, A. N. DeMaria, N. Dib, K. L. Christman, *Sci. Trans. Med.* **2013**, *5*, 173ra25.
[51] N. Merna, K. M. Fung, J. J. Wang, C. R. King, K. C. Hansen, K. L. Christman, S. C. George, *Tissue Eng. Part A* **2015**, *21*, 2195.
[52] K. R. Vrijsen, J. A. Maring, S. A. Chamuleau, V. Verhage, E. A. Mol, J. C. Deddens, C. H. Metz, K. Lodder, E. C. van Eeuwijk, S. M. van Dommelen, P. A. Doevendans, A. M. Smits, M. J. Goumans, J. P. Sluijter, *Adv. Healthcr. Mater.* **2016**, *5*, 2555.
[53] A. van Mil, S. Grundmann, M. J. Goumans, Z. Lei, M. I. Oerlemans, S. Jaksani, P. A. Doevendans, J. P. Sluijter, *Cardiovasc. Res.* **2012**, *93*, 655.
[54] A. B. Aurora, A. I. Mahmoud, X. Luo, B. A. Johnson, E. van Rooij, S. Matsuzaki, K. M. Humphries, J. A. Hill, R. Bassel-Duby, H. A. Sadek, E. N. Olson, *J. Clin. Invest.* **2012**, *122*, 1222.
[55] L. Chen, Y. Wang, Y. Pan, L. Zhang, C. Shen, G. Qin, M. Ashraf, N. Weintraub, G. Ma, Y. Tang, *Biochem. Biophys. Res. Commun.* **2013**, *431*, 566.
[56] J. Krutzfeldt, S. Kuwajima, R. Braich, K. G. Rajeev, J. Pena, T. Tuschl, M. Manoharan, M. Stoffel, *Nucleic Acids Res.* **2007**, *35*, 2885.
[57] L. Barile, V. Lionetti, E. Cervio, M. Matteucci, M. Gherghiceanu, L. M. Popescu, T. Torre, F. Siclari, T. Moccetti, G. Vassalli, *Cardiovasc. Res.* **2014**, *103*, 530.
[58] V. Sokolova, A. K. Ludwig, S. Hornung, O. Rotan, P. A. Horn, M. Epple, B. Giebel, *Colloids Surf. B Biointerfaces* **2011**, *87*, 146.
[59] T. D. Johnson, S. Y. Lin, K. L. Christman, *Nanotechnology* **2011**, *22*, 494015.
[60] K. R. Vrijsen, J. P. Sluijter, M. W. Schuchardt, B. W. van Balkom, W. A. Noort, S. A. Chamuleau, P. A. Doevendans, *J. Cell Mol. Med.* **2010**, *14*, 1064.
[61] F. Arslan, R. C. Lai, M. B. Smeets, L. Akeroyd, A. Choo, E. N. Aguor, L. Timmers, H. V. van Rijen, P. A. Doevendans, G. Pasterkamp, S. K. Lim, D. P. de Kleijn, *Stem. Cell Res.* **2013**, *10*, 301.
[62] J. W. Wassenaar, R. Gaetani, J. J. Garcia, R. L. Braden, C. G. Luo, D. Huang, A. N. DeMaria, J. H. Omens, K. L. Christman, *J. Am. Coll. Cardiol.* **2016**, *67*, 1074.
[63] S. F. Badylak, *Trans. Immunol.* **2004**, *12*, 367.
[64] S. F. Badylak, *Ann. Biomed. Eng.* **2014**, *42*, 1517.
[65] J. L. Ungerleider, T. D. Johnson, N. Rao, K. L. Christman, *Methods* **2015**, *84*, 53.
[66] A. M. Smits, P. van Vliet, C. H. Metz, T. Korfage, J. P. Sluijter, P. A. Doevendans, M. J. Goumans, *Nat. Protoc.* **2009**, *4*, 232.

